Engineering Notes

Aerodynamic Hysteresis of a Low-Reynolds-Number Airfoil

Hui Hu,* Zifeng Yang,† and Hirofumi Igarashi‡
Iowa State University, Ames, Iowa 50011

Introduction

LOW-REYNOLDS-NUMBER airfoil aerodynamics is important for both military and civilian applications. The applications include propellers, sailplanes, ultralight man-carrying/man-powered aircraft, high-altitude vehicles, wind turbines, unmanned aerial vehicles (UAVs), and micro air vehicles (MAVs). For the applications just listed, the combination of small length scale and low flight velocities results in airfoils operating at low chord Reynolds numbers of $Re < 500,000$.

It is well known that many significant aerodynamic problems occur below chord Reynolds numbers of about 500,000. Hysteresis phenomena have been found to be relatively common for round-nosed airfoils at low Reynolds numbers. Aerodynamic hysteresis of an airfoil refers to airfoil aerodynamic characteristics as it becomes history dependent, i.e., dependent on the sense of change of the angle of attack, near the airfoil stall angle. The coefficients of lift, drag, and moment of the airfoil are found to be multiple-valued rather than single-valued functions of the angle of attack. Aerodynamic hysteresis is of practical importance because it produces widely different values of lift coefficient and lift-to-drag ratio for a given angle of attack. It could also affect the recovery from stall and/or spin flight conditions. Whereas aerodynamic hysteresis associated with the pitching motion of airfoils (also known as dynamic stall) has been investigated extensively as summarized in the review article of McCorskey [1], hysteresis phenomena observed for static stall of an airfoil have received much less attention.

Mueller [2] investigated the aerodynamic characteristics of Lissaman 7769 and Miley M06-13-128 airfoils at low Reynolds numbers, and found both airfoils produced hysteresis loops in the profiles of measured lift and drag forces when they operated below chord Reynolds numbers of 300,000. Based on qualitative flow visualization with smoke, he suggested that airfoil hysteresis is closely related to laminar boundary-layer transition and separation on the airfoils. Hoffmann [3] studied the aerodynamic characteristics of a NACA 0015 airfoil at a chord Reynolds number of 250,000, and hysteresis loop was observed in the measured coefficients of drag and

lift. He also found that hysteresis was observed for low-freestream turbulence cases but disappeared for high-freestream turbulence cases. More recently, Mittal and Saxena [4] conducted a numerical study to predict the aerodynamic hysteresis near the static stall angle of a NACA 0012 airfoil in comparison with the experimental data of Thibert et al. [5].

In the present study, we report the measurement results of an experimental study to investigate aerodynamic hysteresis near the static stall angle of a low-Reynolds-number airfoil. In addition to mapping surface pressure distribution around the airfoil with pressure sensors, a high-resolution particle image velocimetry (PIV) system was used to make flowfield measurements to quantify the occurrence and behavior of boundary-layer transition and/or separation on the airfoil when aerodynamic hysteresis occurs. To the best knowledge of the authors, this is the first effort of its nature. The primary objective of the present study is to gain further insight into fundamental physics of aerodynamic hysteresis. In addition, the quantitative flowfield measurements will be used as the database for the validation of computational fluid dynamics (CFD) simulations of such complex phenomena for the optimum design of low-Reynolds-number airfoils.

Studied Airfoil and Experimental Setup

The experiments were performed in a closed-circuit, low-speed wind tunnel located in the Aerospace Engineering Department of Iowa State University. The tunnel has a test section with a 1×1 ft (30×30 cm) cross section and optically transparent walls. The tunnel has a contraction section upstream of the test section with screen structures and a cooling system installed ahead of the contraction section that can provide uniform, low-turbulent incoming flow to the test section.

The airfoil used in the present study is a NASA low-speed GA(W)-1 airfoil [also labeled as NASA LS(1)-0417]. The chord length of the airfoil model is 101 mm, i.e., $C = 101$ mm. The velocity of the incoming flow was set as $U_\infty = 24.0$ m/s, which corresponds to a chord Reynolds number of $Re = 160,000$. The turbulence intensity of the incoming stream was found to be 1.2%, measured by using a hot-wire anemometer. The airfoil model is equipped with 43 pressure taps at its median span, and the pressure taps were connected to a pressure acquisition system (DSA3217, Scanivalve Corp.). The precision of the pressure acquisition system is ± 0.2% of the full scale (± 10 in. H_2O).

A PIV system was used to make flow velocity field measurements along the chord at the middle span of the airfoil. The flow was seeded with ~ 1 μm oil droplets. Illumination was provided by a double-pulsed Nd:YAG laser (NewWave Gemini 200) emitting two pulses of 200 mJ at the wavelength of 532 nm with a repetition rate of 10 Hz. The laser beam was shaped to a laser sheet (thickness ~ 1 mm) by using a set of mirrors, spherical and cylindrical lenses. A high-resolution 12-bit (1376×1040 pixel, SensiCam, Cooke Corp.) charge-coupled device (CCD) camera was used for PIV image acquisition with its axis perpendicular to the laser sheet. The CCD camera and the double-pulsed Nd:YAG lasers were connected to a workstation via a digital delay generator, which controlled the timing of the laser illumination and the image acquisition. Instantaneous PIV velocity vectors were obtained by using a frame-to-frame cross-correlation technique with interrogation windows of 32×32 pixels. An effective overlap of 50% of the interrogation windows was

*Assistant Professor, Aerospace Engineering Department; huhui@iastate.edu. AIAA Senior Member.
†Graduate Student, Aerospace Engineering Department.
‡Undergraduate Student, Aerospace Engineering Department.

employed for the PIV image processing. The effective resolution of the PIV measurements, i.e., grid sizes, is $\Delta/C \approx 0.035$. The time-averaged quantities such as mean velocity (U, V) and normalized turbulent kinetic energy $(\mathrm{TKE} = \frac{1}{2}(\overline{u'u'} + \overline{v'v'})/U_\infty^2)$ distributions were obtained from a cinema sequence of 200 frames of instantaneous velocity fields. The measurement uncertainty level for the velocity vectors is estimated to be within 2.0%, and that of TKE is about 5.0%.

Experimental Results and Discussions

In the present study, the lift and drag coefficients of the airfoil were estimated by numerically integrating the pressure distribution around the airfoil. It should be noted that the drag coefficient of an airfoil is composed of two parts, the pressure drag component (which comes from the fore and aft unbalance in the pressure distribution around the airfoil) and the skin friction component (which comes from the viscous surface stresses around the airfoil). At low angles of attack, skin friction dominates the total drag, whereas the pressure drag component is minor. At high angles of attack, the reverse occurs. Because the skin friction drag component was ignored in the present study, as a result, the drag coefficient of the airfoil was underestimated. The underestimation of the aerodynamic drag could be significant for the cases at low angles of attack. Because aerodynamic hysteresis of an airfoil is usually found to occur at high angles of attack (near airfoil stall angle), the pressure drag component is significant and skin friction drag is negligible when aerodynamic hysteresis occurs. In the present study, all the coefficient data were corrected for wind-tunnel blockages [6].

Figure 1 shows the profiles of the estimated lift and drag coefficients vs angle of attack (AOA). Hysteresis in the aerodynamic coefficients can be observed clearly for the angles of attack lying between 13 and 15 deg. With the increasing angle of attack, airfoil stall was found to occur at AOA = 15 deg, whereas for the decreasing angle, it occurs at AOA = 13 deg. The hysteresis loop was found to be clockwise in the lift coefficient profiles and counterclockwise in the drag coefficient profiles. The hysteresis resulted in significant variations of lift coefficient C_l and lift-to-drag ratio l/d for the airfoil at a given angle of attack. For example, the lift coefficient and lift-to-drag ratio at AOA = 14 deg were found to be $C_l = 1.33$ and $l/d = 23.5$ when the angle is at the increasing angle branch of the hysteresis loop. The values were found to become $C_l = 0.80$ and $L/D = 3.66$ for the same 14 deg angle of attack when it is at the decreasing angle branch of the hysteresis loop.

Figure 2 shows the measured surface pressure coefficient distributions around the airfoil at AOA = 14 deg. Although the surface pressure distribution on the airfoil lower surface do not change very much, the surface pressure distribution on the airfoil upper surface was found to vary significantly when the 14 deg angle of attack is at the increasing angle branch of the hysteresis loop compared with those at the decreasing angle branch. With the AOA = 14 deg at the increasing angle branch, the surface pressure coefficient profile along the airfoil upper surface was found to reach its negative peak rapidly at a location near to the airfoil leading edge, then the surface pressure recovers over the airfoil upper surface. A region of nearly constant pressure (i.e., "plateau" region) was found at the locations of $X/C \approx 0.05 \sim 0.10$ with a sudden increase in surface pressure following the plateau region. According to Ruessell [7], such plateau region followed by a sudden increase in surface pressure would indicate the formation of a separation bubble on the airfoil upper surface in the region of $X/C \approx 0.05 \sim 0.15$. Further downstream of $X/C < 0.15$, the surface pressure was found to recover gradually and smoothly due to the reattachment of the separated boundary layer. With the AOA = 14 deg at the decreasing angle branch of the hysteresis loop, the negative pressure coefficient peak near the airfoil leading edge was found to decrease significantly. The surface pressure over airfoil upper surface was found to be nearly constant. Such surface pressure distribution would indicate that large-scale flow separation has occurred over the airfoil upper surface, i.e., the airfoil is in stall state [7].
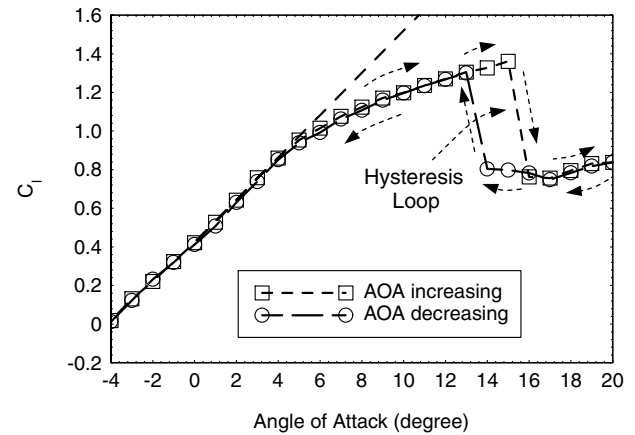
a) Lift coefficient
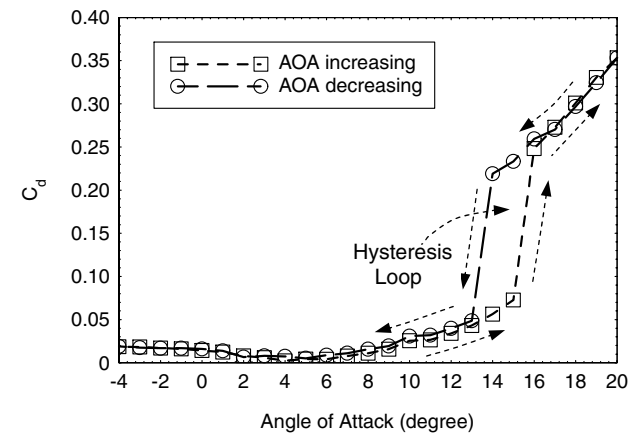
b) Drag coefficient

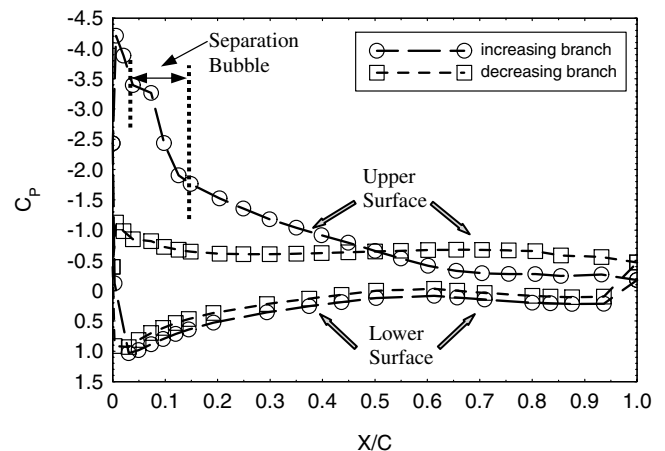Fig. 1   Coefficients of lift and drag vs angle of attack.

Fig. 2   Surface pressure distribution at AOA = 14 deg.

As visualized clearly from the mean velocity vector distributions and the corresponding streamlines given in Fig. 3a, incoming flow streams were found to be able to attach to the airfoil upper surface in general with the 14 deg angle of attack at the increasing branch of the hysteresis loop. The measured surface pressure distribution shown in Fig. 2 indicates that a separation bubble was generated in the region of $X/C \approx 0.05 \sim 0.15$. Because the thickness of separation bubbles generated on low-Reynolds-number airfoils is usually very small, i.e., <1% of the chord length [8], the separation bubble could not be revealed clearly from the PIV measurement results due to the limited spatial resolution of the present PIV measurement (i.e., $\Delta/C = 0.034$). However, the existence of the separation bubble
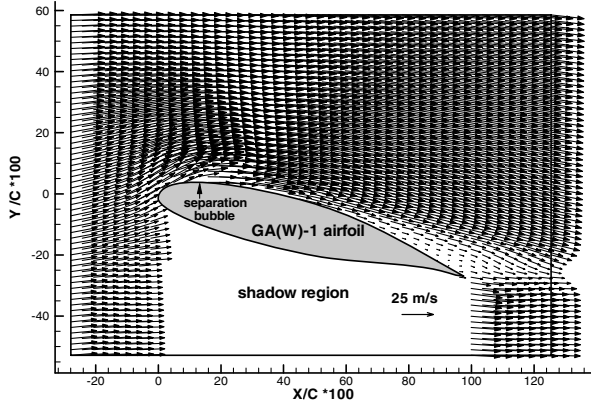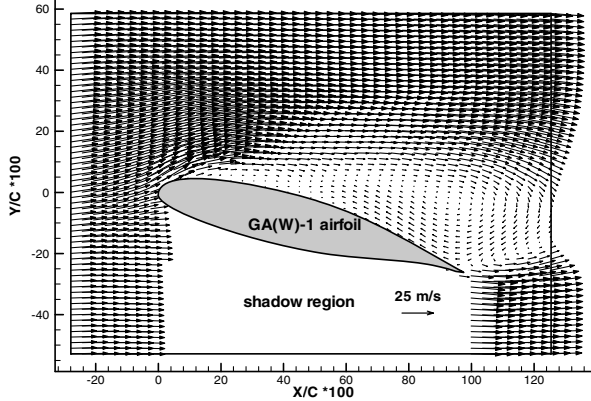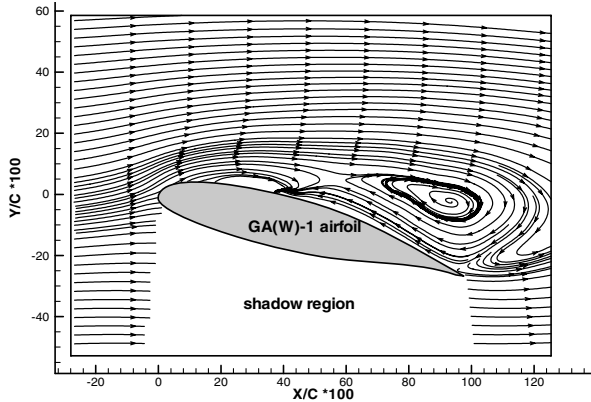
mean velocity vectors
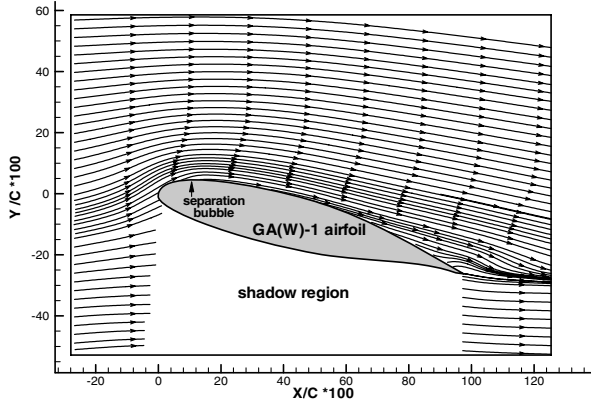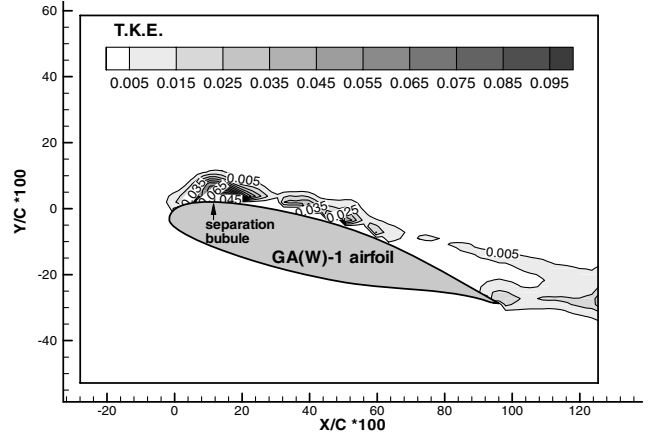

streamlines of the mean flowfield
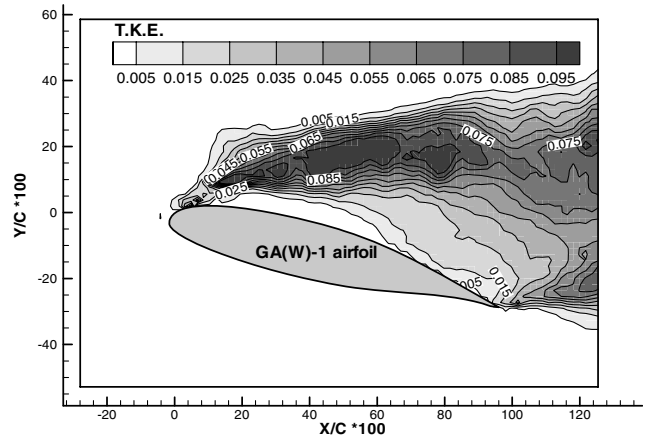
a)

mean velocity vectors

streamlines of the mean flowfield

b)

Fig. 3   PIV measurement results at AOA = 14 deg at the a) increasing and b) decreasing branch of the hysteresis loop.

a) Angle at increasing angle branch

b) Angle at the decreasing angle branch

Fig. 4   Normalized turbulent kinetic energy distributions at AOA = 14 deg.

near the airfoil leading edge can still be seen vaguely from the distributions of the mean velocity vectors and the corresponding streamlines. Because the incoming flowstreams could attach to the airfoil upper surface in general, the wake region downstream of the airfoil is reasonably small. The small wake region would indicate a relatively small aerodynamic drag force acting on the airfoil, which is consistent with the drag coefficient data given in Fig. 1.

Both the mean velocity vectors and the corresponding streamlines shown in Fig. 3b reveal that incoming flowstreams separated from the airfoil upper surface with the 14 deg angle of attack at the increasing angle branch of the hysteresis loop. Large-scale flow separation was found to occur on almost the entire airfoil upper surface, i.e., the airfoil is in stall state. An interesting feature identified from the distribution of the streamlines is that the boundary layer that separated from the airfoil upper surface near the airfoil leading edge seems to try to reattach to the airfoil upper surface at the location of $X/C \approx 0.40$. However, the strong reversing flow from the airfoil trailing edge prevented the separated boundary layer from reattaching to the airfoil upper surface and kept the airfoil in stall state. The flowfield around the airfoil seems to be able to "remember" its past history when the angle of attack changes inside the hysteresis loop. The large-scale flow separation on the airfoil upper surface resulted in a very large circulation region in the wake of the airfoil, which would indicate a significant aerodynamic drag force acting on the airfoil. This was confirmed from the drag force data given in Fig. 1.

Figure 4 shows the normalized turbulent kinetic energy (TKE) distributions around the airfoil at AOA = 14 deg. When the 14 deg angle of attack is at the increasing angle branch of the hysteresis loop, because the incoming flowstream could attach to the airfoil upper surface in general except in the small region near the airfoil leading

edge where separation bubble was formed, the TKE level of the flowfield around the airfoil was found to be relatively low. The region with relatively higher TKE value was found to concentrate in the region where the separation bubble was generated. When the 14 deg angle of attack is at the decreasing angle branch of the hysteresis loop, the boundary layer was found to separate from the airfoil upper surface near the airfoil leading edge as described before. Instantaneous PIV measurement results (not given here) revealed that the separated laminar boundary layer would transit to turbulence rapidly and cause periodic shedding of strong Kelvin–Helmholtz vortex structures. Therefore, the TKE level of the flowfield around the airfoil was found to become significantly higher compared with the case with the 14 deg angle of attack at the increasing angle branch of the hysteresis loop. The regions with higher TKE were found to be along the shedding path of the unsteady Kelvin–Helmholtz vortex structures.

Conclusions

An experimental study was conducted to investigate the aerodynamic characteristics of a NASA low-speed GA(W)-1 airfoil at the chord Reynolds number of $Re = 160,000$. Aerodynamic hysteresis was observed for the angles of attack close to the static stall angle of the airfoil. In addition to mapping surface pressure distribution around the airfoil, a high-resolution PIV system was used to make quantitative flowfield measurements to quantify the occurrence and behavior of boundary layer transition and/or separation on the airfoil when aerodynamic hysteresis occurs. For the same angle of attack, the flow obtained along the increasing angle branch of the hysteresis loop results in an almost attached flow with small unsteadiness, higher lift and lower drag, whereas the one with decreasing angle of attack is associated with large unsteadiness, lower lift, and higher drag. The hysteresis was found to be closely related to the behavior of the laminar boundary-layer transition and/or separation on the airfoil. The ability of the flow to remember its past history is responsible for the hysteretic behavior.

Acknowledgment

References

[1] McCorskey, W. J., "Unsteady Airfoil," *Annual Review of Fluid Mechanics*, Vol. 14, 1982, pp. 285–311.
doi:10.1146/annurev.fl.14.010182.001441

[2] Mueller, T. J., "The Influence of Laminar Separation and Transition on Low Reynolds Number Airfoil Hysteresis," *Journal of Aircraft*, Vol. 22, No. 9, 1985, pp. 763–770.

[3] Hoffmann, J. A., "Effects of Freestream Turbulence on the Performance Characteristics of an Airfoil," *AIAA Journal*, Vol. 29, No. 9, 1991, pp. 1353–1354.

[4] Mittal, S., and Saxena P., "Prediction of Hysteresis Associated with Static Stall of an Airfoil," *AIAA Journal*, Vol. 38, No. 5, 2000, pp. 933–935.

[5] Thibert, J. J., Grandjacques, M., and Ohman, L. H., "Experimental Database for Computer Program Assessment," AGARD, TR AR-138, May 1979.

[6] Rogers, E. W. E., "Blockage Effects in Closed or Open Tunnels," AGARDograph 109, 1966, pp. 279–340.

[7] Ruessell, J., "Length and Bursting of Separation Bubbles: A Physical Interpretation," *Science and Technology of Low Speed Motorless Flight* NASA CP 2085, Pt. 1, 1979.

[8] O'Meara, M. M., and Mueller, T. J., "Laminar Separation Bubble Characteristic on an Airfoil at Low Reynolds Numbers," *AIAA Journal*, Vol. 25, No. 8, 1987, pp. 1033–1041.